Human Tropoelastin Sequence: Dynamics of Polypeptide Coded by Exon 6 in Solution

D. Tintar,[1] V. Samouillan,[1] J. Dandurand,[1] C. Lacabanne,[1] A. Pepe,[2] B. Bochicchio,[2] Antonio M. Tamburro[2]

[1] *Laboratoire de Physique des Polymères, CIRIMAT UMR 5085, Institut Carnot, Université Paul Sabatier, Toulouse, France*

[2] *Department of Chemistry, University of Basilicata, Potenza, Italy*

DOI 10.1002/bip.21282

ABSTRACT:

Calorimetric studies were performed on exon 6 in powdered form and in solution [water and 2,2,2-trifluoroethanol (TFE), a structure-inducing solvent or cosolvent]. Dynamic dielectric spectroscopy (DDS) analyses were realized in water and 20% TFE. The major role of solvent–peptide organization is evidenced with these techniques. Calorimetric measurements reveal the structural water organization around the polypeptide as well as the presence of hydrophobic interactions in TFE solution. Dielectric measurements showed for exon 6/water a decrease of relaxations times of bulk solvent implying a faster dynamics with a slight increase of the activation entropy, suggesting that exon 6 probably creates disorder within the solvent. For TFE/water mixtures, an influence of exon 6 on its environment was seen with a relaxation associated with the exon 6/solvent interactions reinforced by storage of 72 h. Finally, exon 6/solvent interactions were clearly observed with addition of TFE.

Keywords: *dielectric spectroscopy; thermal analysis; elastin*

Correspondence to: V. Samouillan; e-mail: vsamou@cict.fr

This article was originally published online as an accepted preprint. The "Published Online" date corresponds to the preprint version. You can request a copy of the preprint by emailing the Biopolymers editorial office at biopolymers@wiley.com

INTRODUCTION

An important goal concerning elastin research is the revealing of general mechanisms of elastin elasticity. Because of the extreme insolubility of elastin, investigations on the soluble precursor protein called "tropoelastin" are generally carried out. Significant results have been obtained on the structure-function relationships of hydrophobic sequences of tropoelastin.[1] Indeed, analyses by circular dichroism (CD) and nuclear magnetic resonance (NMR) of polypeptide sequences encoding the single exons of human tropoelastin in different solvents evidenced the presence of labile conformations, whose stability is strongly microenvironment-dependent. Within this context, several conformations of exons and notably the exon 6 of human tropoelastin were studied in different solvents with these techniques by Tamburro's group. The results showed the presence of poly-proline II (PPII) conformation in water and α-helix conformation in TFE,[2] emphasizing the influence of the microenvironment on the polypeptide. The polypeptide sequence encoded by exon 6 (exon 6) with the following amino acid sequence: GLGAFPAVTFPGALVPGG VADAAAAYKAAKA can be considered as a "mini elastin" with its hydrophobic part (GLGAFPAVTFPGALVPGG) and its alanine-rich crosslink domain (VADAAAAYKAAKA).[2] The study of single domains of tropoelastin for getting information on the entire protein has been used and validated by previous results.[3] As a matter of fact, this so-called reductionist approach has been repeatedly demonstrated to be able to give significant insights on the elastin structure. The importance of solvent is well known to be essential for the

biological function and notably for the mechanism of elastin elasticity. However, the functional solvent environment for insoluble elastin is difficult to predict. As a matter of fact, the protein hydrophobicity and its highly cross-linked nature suggest a less polar internal environment than the surrounding solvent.

Within this context, investigations were performed by differential scanning calorimetry (DSC) and dynamic dielectric spectroscopy (DDS) on the synthetic polypeptide exon 6, in order to complement the CD and NMR studies. The aim of this study is to investigate the dynamics of exon 6/solvent system both of the mesoscopic and nanometric scale in order to correlate the molecular mobility to the physical structure. Indeed, the study of exon 6 considered as a "mini elastin" according to the solvent is a good example to help the understanding of elastin/environment interactions. The experiments were performed both in water and in 2,2,2-TFE. TFE is a significantly less polar solvent (dielectric permittivity $\varepsilon = 27$ at 20°C) than water and is usually considered as a structure-inducing solvent, favoring folded conformations such as α-helices and β-turns. For the exon 6, CD and NMR studies have showed the presence of PPII conformation in water and α-helix conformation in TFE or water/TFE.[2] DSC has been used to observe the thermal transitions of peptide first in lyophilized state (nonfunctional state) and second in solution (functional state) in order to highlight the effect of solvent on the peptide and also to get information about the physical structure. In our work, DDS has been used to analyze relaxation phenomena and to determine the molecular mobility of the system. Dielectric relaxation is a well-suited method to probe the dynamics of protein solutions.[4]

It is well known that the hydration shell surrounding a protein molecule is constituted by different kinds of water. The properties of water molecules in the vicinity of a biomolecule differ from those of bulk water.[5–7] In the literature, the dielectric studies of proteins in solution in the high-frequency range (from 10^{-2} to 10^{10} Hz) showed different dynamics of waters surrounding the protein.[8–12] Dielectric techniques have shown their ability to define the state of mobility of water molecules at the vicinity of proteins; these results indicate that some water molecules can have a lowered rotational mobility (typical hydration shell), and other water molecules can have a higher mobility than that of bulk water.[13] Recently, another dielectric study on associated dynamics at the secondary structure of several oligo-peptide series was carried out[14] and allowed a localization of helical domains.

Nevertheless, in the higher temperature range, encompassing the physiological condition, conductivity dominates the dielectric response, this phenomenon increasing at low frequency. In the literature, studies using dielectric techniques upon the proteins or polypeptides in solution in their functional state (hydrated state and above 0°C) are generally carried out in the high-frequency range (between MHz and GHz) to reveal the different dynamics of water surrounding the biomolecule (hydration shell) and the intrinsic protein movement. However, very few dielectric studies were carried out in the low-frequency range and below 0°C.[9] In this work, we focused on the low-temperature range, generally associated with bulk solvent relaxations. Thanks to this method, the influence of the exon on its environment has been assessed. In fact, at low temperature, the structure of exon 6 is fixed and the measurements reveal local motions in the solvent, particularly in the last hydration layer. Via this method, we want to point up the last hydration layer around polypeptides. In a general way, the analyses of exon 6 by DSC and DDS can bring additional information on the specific behavior of the solvents around the peptide system.

MATERIALS AND METHODS

Materials

The peptide was synthesized by using an automatic synthesizer APPLIED BIOSYSTEM model 431 A. Fluorenyl-methoxy-carbonyl (Fmoc)/dicyclohexyl carbodiimide (DCC)/hydroxybenzotriazole (HOBt) chemistry was used. The Fmoc-ammino acids were purchased from Nova Biochem (Laufelfingen, Switzerland) and from Inbios (Pozzuoli, Italy). The cleavage of peptide from resin was achieved by using an aqueous mixture of 95% trifluoroacetic acid. 1,2-Ethanedithiol, phenol, and thioanisol were also used in the cleavage mixture when necessary. The peptide was lyophilized and purified by semipreparative and preparative reversed-phase high-performance liquid chromatography. Binary gradient was used and the solvents were H_2O [0.1% trifluoracetic acid (TFA)] and acetonitril (CH_3CN) (0.1% TFA). The purity of peptide was assessed by electrospray mass spectrometry.

Differential Scanning Calorimetry

DSC experiments were performed with a Thermal Analysis Instruments DSC 2920. Calibration was made using indium and cyclohexane as standards. Temperature was adjusted from the analysis of the onset temperature of melting peak of the two standards, resulting in accuracy at ±0.1°C. The cell constant was adjusted from the analysis of the melting peak area of indium, resulting in accuracy of ±0.1 J/g. Two different analyses were carried out by DSC, firstly on powdered peptide and secondly on peptide solutions with two specific solvents (deionized water and TFE).

Concerning powdered peptide (lyophilized exon 6) analyses, samples (1.5–2 mg) were sealed into aluminum pans. Empty pans were used as reference. The experimental protocol applied was a heating rate of 5°C/min from 0 to 230°C with a controlled cooling rate at 10°C/min.

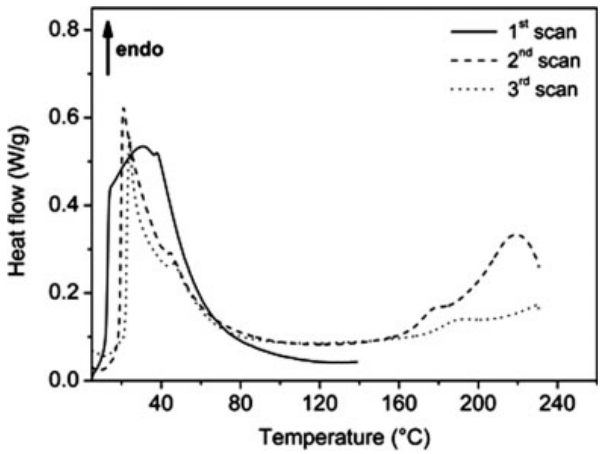

FIGURE 1 DSC thermograms of powdered exon 6 at first (solid line), second (dash line) and third (dot line) scan.

Various concentrations were tested and the selected concentrations for DSC, with a good signal-noise ratio were 100 and 200 mg/ml for water and TFE solvents, respectively. Ten microliters of the corresponding solution were injected inside a hermetic pan. An empty pan was used as reference. Before running the measurements, all samples were maintained at 5°C for 15 min to stabilize the system. The temperature was raised to 60°C at a rate of 5°C/min, after storage for 15 min at 5°C. The rate of cooling depended on the solvent: a rate of −5°C/min in the case of the aqueous solution and a rate of −20°C/min for the TFE solution. The specific cooling rate according to the solvent was used to obtain reproducible successive thermograms.

Turbidimetry Measurements

These measurements were performed using a spectrophotometer Varian Cary 3 equipped with a temperature controller (Varian, Palo Alto, CA). Exon 6 at 1 and 2 mM in 7.5% TFE and in TBS (Tris Buffer Saline) (Tris 50 mM, NaCl 1.5 M, and CaCl2 1.0 mM, pH 7.0) was placed in a quartz cell of 1-cm path length. For the experiment, the use of quartz cuvette required a decrease the percentage of TFE due to its volatility; in this case, 7.5% of TFE was a good compromising. The solution temperature was increased by 2°C steps, and the absorbance was monitored at 440 nm at that temperature after 5 min in order to reach the chosen temperature to obtain the equilibration of the sample. Then the solution temperature was decreased and the absorbance monitored by adopting the previous protocol.

Dynamic Dielectric Spectroscopy

The dielectric analyses were carried out on a Novocontrol BDS 4000 system with an experimental limit for the loss factor tan δ of 10^{-5}. Dielectric measurements were carried out on peptide solutions of 0.5 mg/ml in two solvents: water and water with 20% TFE. The solutions were introduced in glass cell 10-μm thick and set between two stainless steel electrodes. In this case too, the use of glass cell for the experiment required a decrease the percentage of TFE due to its volatility. A sinusoidal voltage of 1 V was imposed. The effective polarized surface of the sample was equal to 100 mm^2. Measurements of the complex dielectric permittivity ε^* were recorded at a given temperature in a frequency range from 10^{-2} to 10^6 Hz. Dielectric isotherm spectra were measured from −150 to 50°C by steps of 5°C. Before each frequency scan, temperature was kept constant to within ±0.2°C.

RESULTS

DSC Analysis: Powdered Exon 6

DSC measurement was performed between 0 and 150°C for the first scan and between 0 and 230°C for the second and third scans. We have reported on Figure 1 the thermogram of each scan. A broad and endothermic peak in the range 0–80°C is observed at the first scan. A step of the heat flow associated with a glass transition phenomenon is detected on the second and third scans at T_g = 172°C and T_g = 184°C, respectively. Moreover, a nonreversible endothermic peak following the glass transition is present at the second scan. Finally, intense and sharp peaks are observed between 20 and 60°C for the second scan and third scans.

DSC Analysis: Exon 6 in Solution

The three DSC thermograms of exon 6 in water at 100 mg/ml are presented in Figure 2. The heat flow versus temperature is plotted from 20 to 60°C for the three scans. The three thermograms exhibit a complex and broad endothermic peak (superimposed with several transitions) with a maximum at 41°C for the first scan and at 45°C for the other scans. In the same way as for the exon 6/water system, we have plotted the heat flow versus temperature of exon 6 in

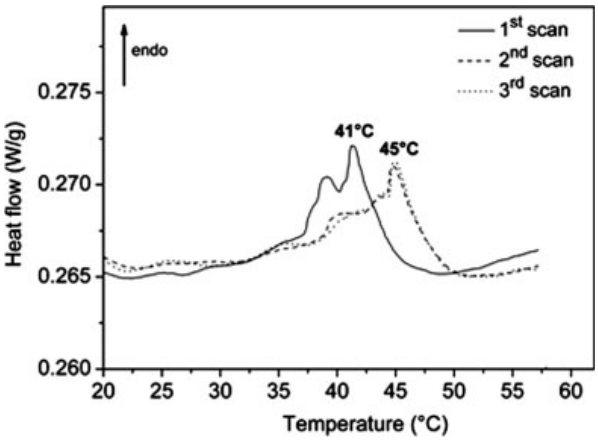

FIGURE 2 DSC thermograms of exon 6 in solution in water at 100 mg/ml at first (solid line), second (dash line), and third (dot line) scan.

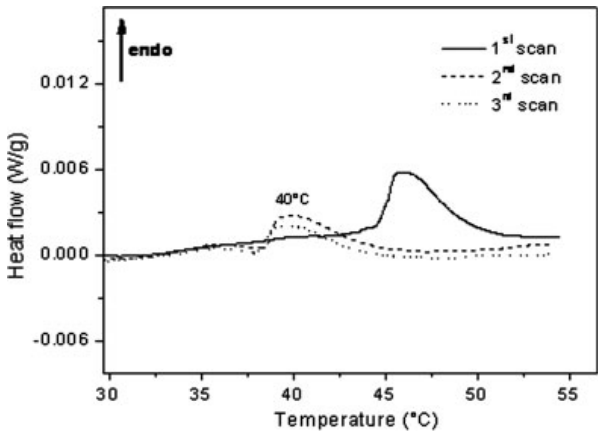

FIGURE 3 DSC thermograms of exon 6 in solution in TFE at 200 mg/ml at first (solid line), second (dash line), and third (dot line) scan.

TFE at 200 mg/ml between 20 and 60°C for the three scans (see Figure 3). A first-order transition of exon 6 in TFE is observed at 47°C on the first thermogram and at 40°C on the second and third thermograms.

Turbidimetry Analysis: Exon 6 in Solution

In Figure 4, turbidimetry an apparent absorbance (TAA) curves as a function of temperature are reported at different concentrations in 7.5% TFE and in TBS. In 7.5% TFE, the typical phase transition is, as expected, dependent on solute concentration and is almost irreversible, therefore indicating

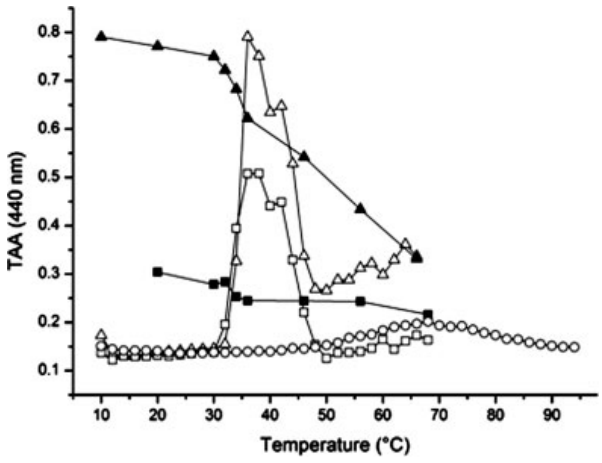

FIGURE 4 Turbidimetry on apparent absorbance curves as a function of temperature for exon 6 in the following conditions: TBS (Tris Buffer Solution), warming curves at 1 mM exon 6 (empty circles); 7.5% TFE, warming curves at 1 mM exon 6 (empty squares) and 2 mM exon 6 (empty triangles); Cooling curves of exon 6 in 7.5% TFE at 1 mM (filled squares) and 2 mM (filled triangles).

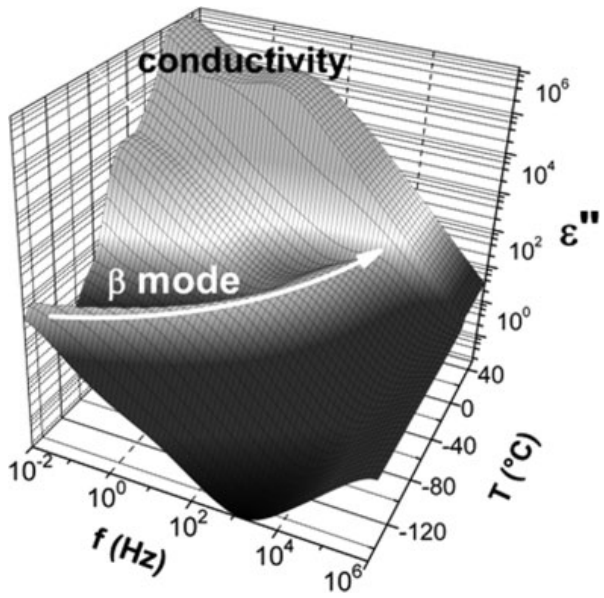

FIGURE 5 Dielectric surface of exon 6 in water at 0.5 mg/ml.

the formation of large aggregates and not of coacervate. In any case, the trend is complex suggesting that different phenomena are occurring. Until around 40°C, the curves are more or less sigmoidal, that is, those expected for a phase transition. However, at higher temperature, a dissociation of the aggregates occurs giving rise to a resulting function with maximum suggesting a possible denaturation process. Concerning the exon 6 in TBS, a slight increase of the curve was seen at around 68°C. This curve clearly indicates the lack of a coacervation phenomenon; at this concentration, the increase of TAA value could be more important with a higher concentration of the polypeptide. As a matter of fact, exon 6 at 100 mg/mL concentration in water solvent gave rise to an irreversible precipitate (data not shown).

DDS Analysis: Exon 6 in Solution

The real (ε') and imaginary parts (ε'') of the complex permittivity of exon 6 in water and mixture with 20% of TFE at 0.5 mg/ml were measured from −150 to 50°C by steps of 5°C. In the higher temperature range (0–50°C), encompassing the physiological condition, conductivity dominates the dielectric response. For this study, we have focused on the relaxation mode at low temperature (−140 to −20°C) and on the variation of the dissipative component ε''. We have plotted in Figures 5 and 6 the variation of ε'' versus frequency and temperature in a three-dimensional plot for the two samples. The ε'' spectra, associated with dissipative phenomena produced during the reorientation of dipoles in their environment, demonstrate localized relaxation at low tempera-

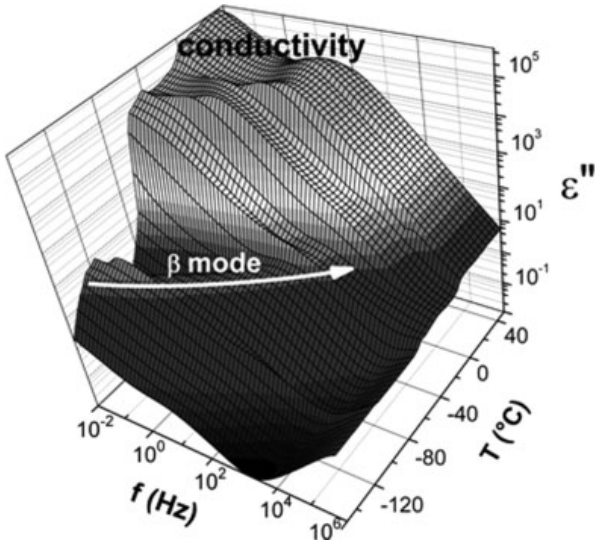

FIGURE 6 Dielectric surface of exon 6 in TFE mixture at 20% in volume at 0.5 mg/ml.

ture that one called β mode (successive spectra following the arrow). A more-detailed observation of the β mode indicates a more restricted temperature range of this mode for the exon 6 in aqueous TFE than for the exon 6 in water. The temperature dependence of these β modes was analyzed by computing the macroscopic relaxation time $\tau_{max} = 1/(2\pi \cdot f_{max})$ related to the maximum of ε'' of each isotherm. These relaxation times have been plotted versus temperature for the exon 6 in water and in aqueous TFE and also for the pure solvents (Figures 7 and 8) in order to compare them.

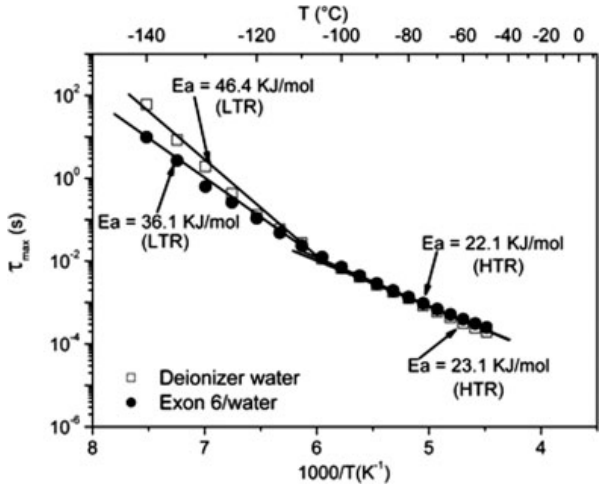

FIGURE 7 Temperature dependence of relaxation timesof the β mode of water and exon 6/water at 0.5 mg/ml (the straight lines in bold correspond to the linear fits).

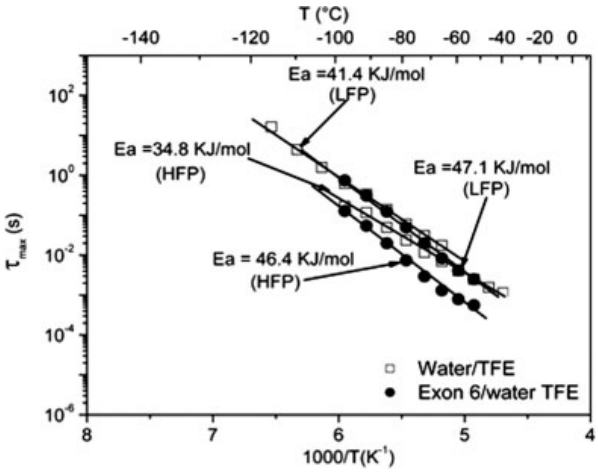

FIGURE 8 Temperature dependence of relaxation times of the β mode of water/TFE at 20% and exon 6/water/TFE at 20% at 0.5 mg/ml (the straight lines in bold correspond to the linear fits).

We noted that τ_{max} follows Arrhenius laws in this temperature zone:

$$\tau_{max}(T) = \tau_0 \exp(E_a/RT)$$

where τ_0 is the preexponential factor, E_a is the activation energy, R is the ideal gas constant, and T is the absolute temperature. The values obtained by linear regressions are reported in Table I where N is the number of experimental points and R the square root of the correlation coefficient. In Figure 5 for water and exon 6/water a single β mode is observed, whom temperature behavior can be separated into two Arrhenius components with a crossover at around -106°C (see Figure 7). Linear fits were carried out to extract

Table 1 Activation Parameters of β Mode for Exon 6 in Solution Computed from DDS Analysis for Low Temperature Relaxation (LTR), High Temperature Relaxation (HTR), Lower Frequency Process (LFP), Higher Frequency Process (HFP)

	τ_0 (s)	E_a (KJ/mol)	N	R
Water	LTR 2.5×10^{-17}	46.4 ± 2.2	7	0.99448
	HTR 7.9×10^{-10}	23.1 ± 0.2	12	0.99964
20% TFE	LFP 1.0×10^{-13}	41.4 ± 0.9	9	0.99862
	HFP 3.2×10^{-12}	34.8 ± 0.9	10	0.99781
Exon 6/water	LTR 5.0×10^{-14}	36.1 ± 1.3	7	0.99714
	HTR 2.0×10^{-09}	22.1 ± 0.4	13	0.99833
Exon 6/water after 2 days	LTR 5.0×10^{-16}	40.5 ± 0.9	7	0.99887
	HTR 5.0×10^{-09}	19.2 ± 0.4	15	0.99723
Exon 6/TFE water	LFP 1.3×10^{-15}	47.6 ± 0.9	8	0.99911
	HFP 5.0×10^{-16}	46.4 ± 1.8	8	0.99579
Exon 6/TFE water after 3 days	HFP 3.2×10^{-15}	43.4 ± 1.1	11	0.99729

the Arrhenius parameters of these two relaxation laws (Table I) for each sample. In both cases, the activation energy for the relaxation observed above −106°C labeled HTR (high-temperature relaxation) is lower than the relaxation below this temperature-labeled LTR (low temperature relaxation). A significant difference is noticed between LTR activation enthalpies of pure water and exon 6/water, the former at 46.4 KJ/mol and the latter at 36.1 KJ/mol (see Table I).

As reported in Figure 6 and highlighted in Figure 8, two distinct relaxations are clearly visible for aqueous TFE and for exon 6 in TFE/water, over a more restricted temperature zone, in comparison with the relaxations shown in Figure 7. The activation energies computed and reported in Table I for aqueous TFE reach higher values for the lower frequency process (LFP) than for the higher frequency process (HFP) one. It is noteworthy that the two activation energies computed for the exon 6 in TFE/water system are higher than the activation energies of the solvent (see Table I and Figure 8), the more significant increase of the activation energy concerning the HFP of exon 6/TFE/water mixture (E_a = 46.4 kJ/mol) compared to HFP solvent (E_a = 34.8 kJ/mol).

The same dielectric measurement was achieved on the exon 6 in solution in water and in TFE/water mixture stored at 4°C for 2 and 3 days for exon 6 in water and in TFE mixture, respectively. Results of DDS analysis and computed temperature dependence are reported on Figures 9 and 10. We have superimposed the relaxation times versus temperature for the stored and nonstored samples to compare them. Arrhenius-like behaviors are evidenced for the variation of τ_{max}. The values obtained from the linear regression of log

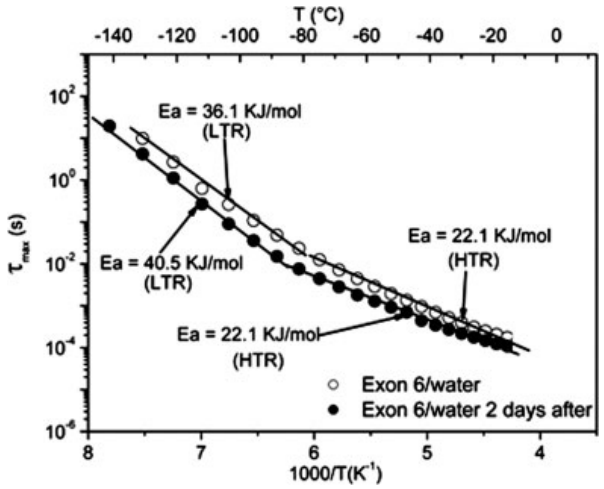

FIGURE 9 Temperature dependence of relaxation times of the β mode at 0.5 mg/ml for exon 6/water and exon 6/water stored during two days at 4°C (the straight lines in bold correspond to the linear fits).

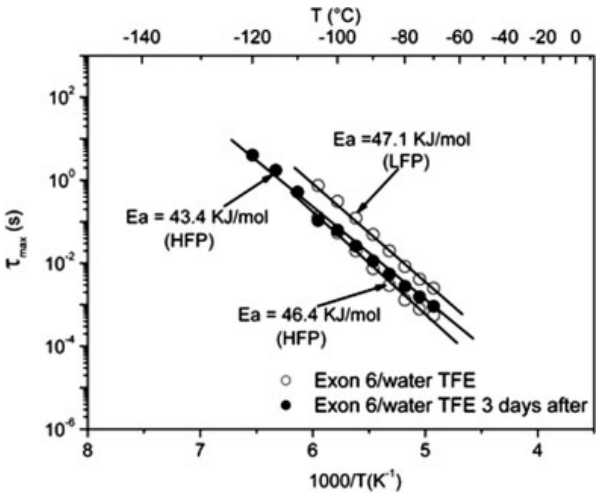

FIGURE 10 Temperature dependence of relaxation times of the β mode at 0.5 mg/ml for exon 6/water TFE at 20% and exon 6/water TFE at 20% stored during three days at 4°C (the straight lines in bold correspond to the linear fits).

$\tau_{max} = f(1/T)$ for the stored samples are reported in Table I. In Figure 9, the same observations were made as those reported in Figure 7. Indeed, the two relaxations observed for pure water and exon 6 in water are also present for the stored exon 6 in water after two days at 4°C in a large temperature zone. In this case too, we note an activation energy for the relaxation of stored exon 6/water below −109°C (LTR) lower than the activation energy of the pure solvent relaxation (Table I and Figure 9). In Figure 9, it is interesting to point out that the relaxation times for the stored sample are slightly lower than the relaxation times of nonstored sample (exon 6/water). In Figure 10, contrary to the two relaxations observed for the nonstored sample of exon 6/TFE/water, a single relaxation mode is present for the stored sample (exon 6/TFE/water after 3 days) with a decreased activation energy of 46.4–43.4 kJ/mol for the HFP of nonstored and stored samples, respectively (Table I and Figure 10).

DISCUSSION

Transitions in the Solid State

The broad endothermic peak observed at the first scan may be considered as a first-order transition, commonly observed in a broad class of hydrated biopolymers. By analogy with previous works,[15] this endothermic event is essentially attributed to the vaporization of bound water. The intense and sharp transition observed after the vaporization of bound

water and localized between 20 and 60°C at the second and third scans was not detected in the thermograms of dry κ-elastin or pentapeptide sequences of elastin.[16,17] It is reported in the literature that a similar peak is observed in lyophilized biological macromolecules such as globular proteins, enzymes, and polysaccharides, between 20 and 40°C irrespective of the kind of proteins, vanishing with increasing water content.[18] According to combined DSC and ^{1}H NMR studies, this endothermic transition could be related to the release of the cooperative motions of water and biological molecules. This endothermic peak certainly originates from the structural changes of the systems with some kinds of weak interactions of exon 6 and water, though the structure of weak interactions is not yet clear. The presence of the glass transition at 172 and 184°C underlines the fact that exon 6 possesses an amorphous zone like elastin. The temperature of this transition is close to the dehydrated elastin glass transition temperature (recorded between 200 and 203°C).[16,19] Previous DSC studies of insoluble elastin performed from the lyophilized state to the hydrated one allowed us to connect the nonfunctional state to the functional one.[19] The main influence of solvent is a shift of the glass transition from 200°C to 0°C, showing that the structure is maintained between the nonfunctional state and the functional state. In spite of the loss of viscoelasticity at physiological temperature, traducing a loss of functionality, the structure is preserved by freeze-drying. The irreversible transition observed in the high-temperature range is probably due to the disruption of intramolecular hydrogen bonds involving a loss of the structure of powdered exon 6. Therefore, the transition may be associated with a denaturation peak as observed for several freeze-dried proteins.[20] The DSC study showed the presence of different structures of powdered exon 6 in its nonfunctional state (dehydrated state). The thermograms revealed the presence of amorphous zones via the glass transition phenomenon and ordered zones via the denaturation event.

These analyses showed similarities between the functional and nonfunctional states with the presence of ordered and disordered sequences in the hydrated state (with studies carried out by CD and NMR). Even if the dehydrated state corresponds to a nonfunctional state, because water is necessary to provide elasticity to elastin or derived-polypeptides, this thermal study shows the presence of structures in exon 6. Similar results were obtained on bovine elastin by FTIR and near infrared Fourier transform,[21] evidencing the presence of secondary structures (β-sheets) in the solid state for elastin, correlated with CD data in solution. In our case, this DSC study in the solid state can be helpful to determine the role of solvent on exon 6. The screening effect of solvent is avoided by studying the solid state, allowing us to get more information on the structure of exon 6, preserved during freeze-drying as observed for a wide variety of proteins.[17,19]

Transitions in Solution

The thermograms of exon 6 in water solution (100 mg/ml) show a first-order endothermic transition that shifts toward high temperatures after a second and a third scan. The thermal response of exon 6 in water (100 mg/ml) is drastically different from the one observed in the solid state and previously described. The several shoulders on the main transition associated with several endothermic events evidence a multiple and complex transition. These complex endothermic phenomena may be due to the successive breaking of hydrogen bonds in the system exon 6/water. Indeed, water by its polar nature possesses in the absence of any solute, labile hydrogen network, which drastically changes around any solute. The various noncovalent links that contribute to the conformational stability of proteins in solution result not only from interactions between the polar and nonpolar groups of the molecule, but also from interactions between these groups and solvent. Moreover, the PPII structure, which is the main conformation of exon 6 in water as demonstrated by CD experiments, is well known to maximize its interactions with water.[22] Unlike α-helices and β-sheets, there are no characteristic backbone hydrogen bonds in PPII. Detecting this secondary structure can be problematic often leading to their mistaken assignment as random coils.[23] Moreover, the unfolding of PPII is locally driven and therefore highly noncooperative.[24] So, a DSC endotherm cannot be assigned to the PPII (random coil transition. On the base of turbidimetry analyses of exon 6 in water, we can suggest that the complex endothermic events are due to the disruption of water organization surrounding the polypeptide, which was shown to form a hydrogel at room temperature. As a result, the endothermic event observed for exon 6 systems could be due to the disorganization of the structural water layer, as previously observed for different proteins in solution. Previous studies concluded that the system constituted by protein and its hydrated layer behave as a highly interconnected phase in the thermodynamic sense.[25]

For the exon 6 in TFE (200 mg/ml), a different thermal response is observed in calorimetric experiments. An observation can be made in Figure 3 on the intensity variation of the transition. This difference in the intensity between the first and the others scans can be explained by the cooling rate effect. In fact, only a fast cooling of the sample (−20°C/min) was shown to result in reproducible thermograms. Previous CD experiments showed that the α helix is the preferred

conformation of exon 6 in TFE, a structure-inducing solvent that strengthens electrostatic interactions. In this case, contrary to the PPII structure, intermolecular bonds stabilize the α helix, which is more compact than the extended PPII helix (signal divided by 10 when compared with water/exon 6). The specially marked effect of TFE on protein structure has been attributed to the formation of relatively large micelle like clusters of alcohol molecules resulting in a higher local alcohol concentration.[26] The weak endothermic transition in the DSC can be reasonably attributed to the disruption of hydrophobic interactions of TFE in the vicinity of α-helices, which will drive to the decrease of α-helices ratio with temperature increasing as shown by CD experiments.[2]

These hypotheses are in good agreement with the results obtained on the apparent absorbance of exon 6/solvent systems. As shown on Figure 4 for exon 6 in 7.5% TFE, with an increase of temperature, a first (inverse temperature) transition occurs, characterized by hydrophobic (entropy-driven) intermolecular interactions resulting in large aggregates. At higher temperatures, enthalpy becomes dominant and a denaturation process occurs that destroy the helical structures (stabilized by intrachain, enthalpy-driven hydrogen bonds) and also the intermolecular hydrophobic bonds which, on their turn, stabilize the large aggregates. At lower concentrations, the aggregates are irreversibly lost, while at higher concentrations, they are irreversibly formed, according to the different cooling curves reported in Figure 4.

Localized Relaxations in Solution

The dielectric experiments performed at low temperature in a protocol that allows the solvent/peptide system to be fixed were useful to get an insight into the organization of solvent in the vicinity of the peptide. The activation energies of two dielectric relaxations observed for pure ice are in good agreement with literature values.[27–30] The observed crossover at −106°C is due to the different type of crystalline defects produced in the ice at higher and lower temperature. According to the literature, the relaxation above −106°C (HTR) for pure water and water/exon 6 systems is probably due to the reorientation of the L defects (doubly unoccupied bonds) caused by impurities. The relaxation below −106°C (LTR) was previously addressed to intrinsic defects of ice because of the gradual precipitation of dissolved impurities at low temperature. Therefore, the activation energy rises, because the energy required to produce the defects increases.[31,32] However, the relaxation below −106°C is a matter for debate. Focusing on the activation energy parameters, an influence of exon 6 can be demonstrated by the solvent relaxation. The presence of exon 6 decreases the activation energy of the intrinsic defect of the ice (Table I). In this case, the origin of the relaxation below −106°C agrees with the experimental results, because the addition of exon 6 to water may be considered as equivalent to the presence of impurities. Nevertheless, it is noteworthy that each kind of impurity acts in a distinct way. Dielectric studies on the effect of dopants such as alkali hydroxides on ice molecular relaxation have showed a drastic fall of relaxation times,[33] showing a different comportment with such impurities.

Moreover, the relaxation times τ_{max} of the LTR processes slightly decrease with addition of exon 6: this more rapid dynamics could be associated with the hydration shell around the peptide, with an organization distinct from bulk water. Reorientation of H-bonds defects in this case could be facilitated, as shown by the enthalpy decrease and the by the drop of relaxation times.

As a time-dependant effect was observed by calorimetric studies, we have studied exon 6 in water after storage at 4°C for 2 days (see Figure 9). To see the influence of the storage, we compared the evolution of relaxation times with the non-stored sample. The same behavior has been noticed for both samples with a crossover between the two relaxations at −109°C for the stored sample. The relaxation times of stored sample are slightly lower than the relaxation times of non-stored sample. The decrease of τ_{max} implies a faster dynamics due to more localized interactions between water molecules and peptide, which are stabilized during time. This behavior has been observed for different polypeptides in solution by dielectric measurements and described as a "hyper-mobile" state of water.[13] According to the Eyring's theory, $\tau_0 = h(kT)^{-1} \exp(-\Delta S/R)$ (where ΔS is the activation entropy, h is Planck's constant, and k Boltzmann's constant), we can deduce a slight increase of ΔS. As a matter of fact, interactions between water molecules and peptide are generated, and thus an increase in the number of possible activated states is observed during the dipolar reorientation. The slight increase of ΔS during storage leads us to suppose that the disorder observed in the environment may be due to the increase of the number of waters/peptide interactions during the stabilization. So, we can assume that exon 6 creates disorder at the solvent level, with the creation of a hydration shell around the PPII/unordered structure of exon 6.

A clear change of the dielectric response is noticed in the presence of 20% TFE when compared to the dielectric response of pure water. TFE as water cosolvent is known to act as a chaotropic substance, that is, it alters the local ordering of water.[34] It was previously shown by CD experiments that 20% TFE favors the α-helix conformation for exon 6. Two distinct relaxations at HFP and LFP, respectively, are observed in Figure 8. If we focus on the activation energies of

the two relaxations, an influence of exon 6 on the solvent relaxation is seen giving rise to an increase of activation energies (Table I). The more pronounced influence of the exon 6 with a significant increase of the activation energy is noticed for the HFP. These experimental results have allowed us to assign the HFP to interactions between exon 6 and solvent and the LFP to the solvent alone. So, the evolution of HFP mode could traduce the hydrophobic interaction disturbance at the vicinity of exon 6.

To demonstrate the effect of storage in this case too, we have studied the exon 6 in TFE/water mixture stored at 4°C for 3 days (see Figure 10). A significant evolution of the dielectric response has been observed. First, the disappearance of the LFP associated with the solvent. Second, a broader HFP in the extended temperature range, attributed to the interactions between exon 6 and the solvent. The dielectric experiments suggest that the storage favors exon 6/solvent interactions. Indeed, the disappearance of the LFP makes us suppose that the stabilization of exon 6 solvent system promotes the evolution of interactions between peptide and solvent, so favoring the relaxation associated with interactions between exon 6 and solvent (HFP). So, the dielectric experiments on exon 6/TFE water mixture have allowed us to detect an influence of exon 6 on its microenvironment via the increase of activation energies. Furthermore, the attribution of HFP to the interactions between exon 6 and the solvent can be confirmed by the storage, which favors these interactions.

CONCLUSION

Exon 6 in the solid state and in aqueous/TFE solutions was characterized. For the powdered exon 6, ordered (endothermic transition of first order) and disordered zones (pseudo-transition of second order) were observed. These results in the nonfunctional state (lyophilized state) show that exon 6 considered as a "mini elastin" with hydrophobic and cross-link domains possesses its proper organization, with some analogous features as lyophilized elastin.

The major role of solvent and the peculiar solvent-peptide organization is demonstrated with thermal and dielectric measurements in solution. At the mesoscopic scale reached by calorimetric measurements, the organization of water around PPII/unordered conformation was shown, and the hydration shell can be considered as hydrogen bonds network behaving as a phase in a thermodynamic sense. In pure TFE, the solvent shell is mainly constitutes by hydrophobic interactions, which maintain α helices up to 50°C.

At the nanometer scale reached by dielectric measurements, we scan the peculiar solvent shell dynamics around the peptide. An influence of exon 6 on its environment was seen with a decrease of relaxation times (τ_{max}) implying a more rapid dynamics of defects in hydrogen bonds network and at the same time the slight increase of the activation entropy. This observation leads us to suppose that the exon 6 creates slight disorder within the solvent, probably due to the increase of interactions number between water/peptide (hydrogen links) during the stabilization. For the study of exon 6 in TFE/water mixture, a major influence of exon 6 on its environment was seen, with a relaxation process associated with the exon 6/solvent interactions reinforced by the equilibrium at 4°C during 72 h. In a general way, exon 6/solvent interactions were clearly observed with the addition of TFE.

Accordingly, this study gives an idea of the interactions between the solvent, the cosolvent, and the peptide. The knowledge of the property-structure relationships of the exon requires the understanding of mutual influence of environment on peptide and vice versa. It is a basis to help us to resolve the still largely unanswered question: "How the solvent dynamics are affected by the interactions at the peptide surface and how the solvent influences the peptide dynamics?" The study of a more hydrophobic exon such as exon 24 would be interesting to understand hydrophobicity/conformation relationship of certain protein such as elastin. This analysis opens new perspectives for the quantitative study of elastin/environment interactions.

Moreover, our experimental results will be useful for the assessment of starting conditions in molecular dynamics simulations, allowing a better knowledge of solute/solvent interactions. As a whole, the results reported in this work further confirm the validity of the "reductionist approach" and are in agreement with the general description of the elastin structure and dynamics previously published[1,2] by some of us.

REFERENCES

1. Tamburro, A. M.; Bochicchio, B.; Pepe, A. Biochemistry 2003, 42, 13347–13362.
2. Tamburro, A. M.; Pepe, A.; Bochicchio, B. Biochemistry 2006, 45, 9518–9530.
3. Mackay, J. P.; Muiznieks, L. D.; Toonkool, P.; Weiss, A. S. J Struct Biol 2005, 150, 154–162.
4. Nandi, N.; Bhattacharyya, K.; Bagchi, B. Chem Rev 2000, 100, 2013–2045.
5. Pethig, R. Annu Rev Phys Chem 1992, 43, 177–205.
6. Rupley, J. A.; Careri, G. Adv Protein Chem 1991, 41, 37–172.
7. Kuntz, I. D., Jr.; Kauzmann, W. Adv Protein Chem 1974, 28, 239–345.
8. Nandi, N.; Bagchi, B. J Phys Chem B 1997, 101, 10954–10961.

9. Sun, M.; Pejanovic, S.; Mijovic, J. Macromolecules 2005, 38, 9854–9864.
10. Hayashi, Y.; Shinyashiki, N.; Yagihara, S.; Yoshiba, K.; Teramoto, A.; Nakamura, N.; Miyazaki, Y.; Sorai, M.; Wang, Q. Biopolymers 2002, 63, 21–31.
11. Yoshiba, K.; Teramoto, A.; Nakamura, N.; Shikata, T.; Miyazaki, Y.; Sorai, M.; Hayashi, Y.; Miura, N. Biomacromolecules 2004, 5, 2137–2146.
12. Miura, N.; Asaka, N.; Shinyashiki, N.; Mashimo, S. Biopolymers 1994, 34, 357–364.
13. Kabir, S. R.; Yokoyama, K.; Mihashi, K.; Kodama, T.; Suzuki, M. Biophys J 2003, 85, 3154–3161.
14. Papadopoulos, P.; Floudas, G.; Klok, H. A.; Schnell, I.; Pakula, T. Biomacromolecules 2004, 5, 81–91.
15. Samouillan, V.; Dandurand-Lods, J.; Lamure, A.; Maurel, E.; Lacabanne, C.; Gerosa, G.; Venturini, A.; Spina, M. J Biomed Mater Res 1999, 46, 531–538.
16. Samouillan, V.; Dandurand, J.; Lacabanne, C.; Hornebeck, W. Biomacromolecules 2002, 3, 531–537.
17. Megret, C.; Lamure, A.; Pierraggi, M. T.; Lacabanne, C.; Guantieri, V.; Tamburro, A. M. Int J Biol Macromol 1993, 15, 305–312.
18. Takizawa, T.; Nakata, Y. Thermochim Acta 2000, 352, 223–231.
19. Samouillan, V.; André, C.; Dandurand, J.; Lacabanne, C. Biomacromolecules 2004, 5, 958–964.
20. Pikal, M. J.; Rigsbee, D. R.; Roy, M. L. J Pharmaceut Sci 2007, 96, 2765–2776.
21. Debelle, L.; Alix, A. J. P.; Jacob, M. P.; Huvenne, J. P.; Berjot, M.; Sombret, B.; Legrand, P. J Biol Chem 1995, 270, 26099–26103.
22. Carvajal, P. A.; Lanier, T. C. In Water and the Cell; Pollack, G. H.; Cameron, I. L.; Wheatley, D. N., Eds.; Springer: Netherlands, 2006; pp 235–251.
23. Bochicchio, B.; Tamburro, A. M. Chirality 2002, 14, 782–792.
24. Creamer, T. P. Proteins 1998, 33, 218–226.
25. Tompa, K.; Bánki, P.; Bokor, M.; Kamasa, P.; Lasanda, G.; Tompa, P. Biophys J 2009, 96, 2789–2798.
26. Hong, D. P.; Hoshino, M.; Kuboi, R.; Goto, Y. J Am Chem Soc 1999, 121, 8427–8433.
27. Johari, J. P.; Jones, S. J. J Chem Phys 1975, 62, 4213–4223.
28. Kawada, S. J Phys Soc Jpn 1978, 44, 1881–1886.
29. Kawada, S. J Phys Soc Jpn 1979, 47, 1850–1856.
30. Johari, G. P.; Jones, S. J. Proc Roy Soc A 1976, 349, 467–495.
31. Johari, G. P.; Whalley, E. J Chem Phys 1981, 75, 1333–1340.
32. Johari, G. P.; Jones, S. J. Int Conf Phys Chem Ice 1972, 9–12.
33. Tyagi, M.; Murthy, S. S. N. J Phys Chem 2002, 106, 5072–5080.
34. Moelbert, S.; Normand, B.; Rios, P. D. Biophys Chem 2004, 112, 45–57.